

Experimental Fermi Surfaces of Clean and Hydrogen-Covered W(110)

R. H. Gaylord,^(a) K. H. Jeong, and S. D. Kevan

Physics Department, University of Oregon, Eugene, Oregon 97403

(Received 26 August 1988; revised manuscript received 3 March 1989)

Angle-resolved photoemission measurements of the Fermi surfaces of several surface localized states of clean and hydrogen-covered W(110) are reported. Three hole orbits and one electron orbit have been characterized. The hole-orbit states are rapidly attenuated by hydrogen, while the electron-orbit states are shifted to higher binding energy resulting, initially, in an expansion of the Fermi surface, and ultimately, in its conversion to two hole orbits. These data represent the most detailed study of the behavior of the two-dimensional Fermi surface to date.

PACS numbers: 79.60.Gs, 63.20.Kr, 68.35.Rh, 71.25.Hc

The behavior of the Fermi surface has important ramifications for the understanding of a variety of phenomena such as phonon behavior, optical properties, and phase stability. The measurement of the Fermi surfaces of bulk, three-dimensional (3D) systems by techniques utilizing such phenomena as the de Haas-van Alphen effect or the magnetoacoustic effect is well understood and a number of such measurements have been reported in the literature.¹⁻⁵ Unfortunately, the techniques commonly used to measure Fermi surfaces are not readily applied to two-dimensional (2D) states which exist on surfaces and at interfaces, although exceptions to this do exist.⁶

As the dimensionality of a system is reduced to 2D or 1D, the Fermi-surface morphology can have even more pronounced influence on macroscopic observables than it does for a 3D system^{7,8} since singularities in momentum- and energy-dependent screening are more severe. While very little experimental information is available, there is considerable interest in the behavior of the Fermi surface of 2D systems. For example, the reconstructions of W(100) and Mo(100) may result, in part, from phonon anomalies introduced by the morphology of the Fermi surface.⁹⁻¹¹ In addition, coupling of phonons and other low-energy excitations to the electron-hole pair continuum may yield interesting behavior such as Kohn anomalies in the phonon dispersion relations.¹² Recent He-atom scattering experiments^{13,14} have proposed the existence of such anomalies for surface phonons.

In this Letter, we report detailed measurements of the Fermi surfaces of several surface localized states of W(110) by angle-resolved photoemission (ARP). Also, the changes that occur upon adsorption of hydrogen are reported and are discussed in terms of possible phonon anomalies and the hydrogen-induced reconstruction of the surface.^{15,16}

A clean, well-ordered W(110) surface was prepared as described previously.¹⁷ A typical photoemission spectrum could be measured using the ARP system^{18,19} at the National Synchrotron Light Source in 2 to 5 min. Overall operating resolutions were 80 meV (FWHM)

and 0.5° – 1° (FWHM). The crystal was rapidly heated to thermally desorb residual surface contaminants (CO, H) every 5–10 min. The operating pressure was $(0.8\text{--}1.2)\times 10^{-10}$ Torr. Hydrogen was dosed as H₂ at room temperature.

Figure 1 shows spectra from an angular scan along the $\bar{\Delta}$ line ($\bar{\Gamma}$ – \bar{N} , see Fig. 2) of the surface Brillouin zone at a photon energy of 20 eV. This scan represents a variation of k_{\parallel} from 0.50 to 1.14 \AA^{-1} . We call attention to the two peaks indicated by the guidelines. As one moves to larger values of k_{\parallel} these peaks disperse to lower binding energy and cross the Fermi level at 0.84 and 1.1 \AA^{-1} , respectively. These crossings define Fermi-surface points along the $\bar{\Delta}$ line for two distinct states. By making small changes in k_{\parallel} as the Fermi-surface crossing of a state was determined, it was possible to map the 2D Fermi surface throughout the surface Brillouin zone (SBZ). We acknowledge some uncertainty in the precise value of k_{\parallel} at which the crossing occurs due to the width of the state. The accuracy of the measured location of the Fermi-surface contours is primarily limited by this uncertainty. A "worst-case" estimate sets a range of $\pm 0.03 \text{ \AA}^{-1}$ on the measured location of the Fermi surfaces. This is comparable to the precision of the measurement which was $\pm 0.02 \text{ \AA}^{-1}$.

Figure 2 summarizes the results of our measurements for the (a) clean and (b) hydrogen-saturated surfaces. The actual measurements generally only included points in one irreducible wedge of the SBZ with some checks for symmetry in other portions of the zone. The complete Fermi surfaces are, therefore, deduced by symmetry. All of the experimentally deduced Fermi-surface points shown are due to states which are localized at the surface. By surface localized states we refer to both pure surface states, as well as states which are resonant with bulk states. These states are characterized by a lack of dispersion with k_{\perp} , and sensitivity to hydrogen adsorption, either in the form of attenuation or in the form of a change in binding energy. Also shown in this figure is a projection of the bulk Fermi surfaces. These surfaces were produced by direct projection of the de Haas-van

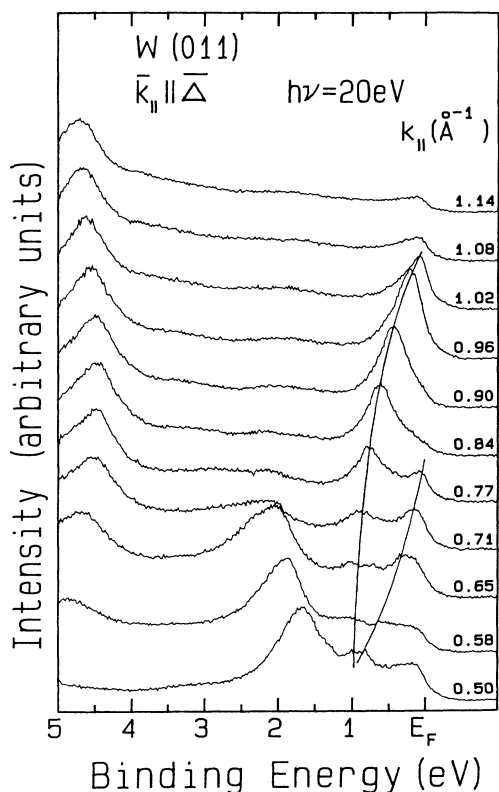


FIG. 1. Series of spectra for the clean W(110) surface resulting from variation of k_{\parallel} from 0.50 to 1.14 \AA^{-1} along $\bar{\Delta}$ with $\mathbf{A} \parallel \bar{\Delta}$ and $\hbar\omega = 20 \text{ eV}$.

Alphen results of Girvan, Gold, and Phillips⁵ onto the (110) SBZ.

For the clean surface, both electron and hole orbits are observed. An electron orbit, centered about $\bar{\Gamma}$, extends across the first SBZ boundary line $\bar{P}-\bar{H}$ and, for the most part, surrounds the projected bulk electron jack. Three distinct hole orbits exist; one is centered around $\bar{\Gamma}$, the second is located symmetrically on the line $\bar{P}-\bar{N}-\bar{P}$, and the third is located on the line $\bar{P}-\bar{H}$. All three hole orbits surround the projections of bulk hole ellipsoids which are centered at the \bar{N} points of the bulk Brillouin zone. These bulk hole ellipsoids project onto three separate regions of the SBZ. The first is located along the edge of the SBZ between \bar{H} and \bar{P} . The surface hole orbit around this bulk projection is located in a true gap and is thus a surface state. At the \bar{N} and $\bar{\Gamma}$ points, projections of the ellipsoids are embedded in projections of the bulk hole octahedra and the bulk electron jack, respectively. The surface hole orbits are also embedded in these projections and are thus resonances. The observation of these well-defined resonances is, in some cases, related to the spin-orbit interaction,²⁰ and will be considered in detail in a forthcoming publication.²¹

The adsorption of hydrogen onto this surface affects the hole-orbit states and the electron-orbit states

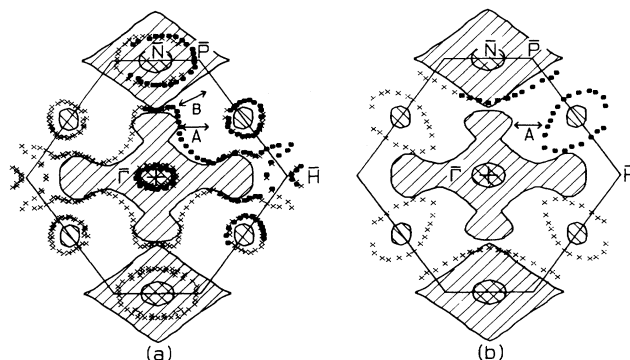


FIG. 2. Fermi surfaces of (a) clean and (b) hydrogen-saturated W(110). The cross-hatched regions result from projection of the bulk Fermi surfaces of Ref. 5; solid circles represent actual data and crosses represent points deduced by the symmetry operations of the surface. (Scale: $\bar{\Gamma}-\bar{N}=1.407 \text{ \AA}^{-1}$.)

differently. The hole-orbit states are rapidly attenuated by hydrogen, while the electron-orbit states simply shift to higher binding energy. The binding-energy shift of the state associated with the electron orbit manifests itself in a dramatic expansion of the Fermi surface. The expansion ultimately results in contact of the Fermi surfaces of neighboring SBZ's in the vicinity of the line "B" of Fig. 2(a), with the consequent production of two hole orbits centered on the $\bar{P}-\bar{N}-\bar{P}$ and $\bar{P}-\bar{H}$ lines as shown in Fig. 2(b).

An experimental determination of the change in the magnitude of the 2D Fermi-surface wave vector (k_F) along the line "A" of Fig. 2 as a function of the work-function change (upper axis) and of the corresponding hydrogen coverage²² (lower axis) is shown in Fig. 3.

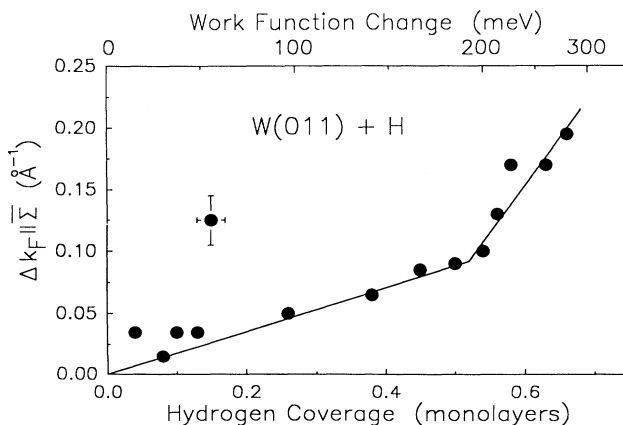


FIG. 3. Change in the Fermi wave vector along the line A of Fig. 2 vs the hydrogen coverage. Upper abscissa indicates the work-function change deduced by measurement of the change in kinetic energy of the secondary tail observed in photoemission. (Note that the scale is not linear over whole range.)

The variation of k_F exhibits two distinct linear regimes with a definite change in slope near a coverage of 0.5 monolayer. This is very close to the coverage at which the hydrogen-induced reconstruction of this surface commences.^{15,16} The break point in the coverage dependence can also be associated with a comparable break point in the initial-state energy of a band associated with this Fermi surface at initial-state energies removed from the Fermi energy.²³ This is the first observation of such a dramatic connection between Fermi-surface morphology, the work-function change, and the surface geometric structure.

It is interesting to speculate that the hydrogen-induced reconstruction of this surface may be directly related to the behavior of the Fermi surface which we have observed here. The proposed model for this reconstruction involves a uniform, lateral shift of the top-layer atoms^{15,16} and may therefore be characterized by a wave vector of $\mathbf{q}=0$. The Fermi surfaces which are centered in neighboring zones are observed to merge along the line B of Fig. 2 as they expand due to hydrogen adsorption, and although the measurement is more difficult in such a region, we also observe a linear variation of the change of the Fermi wave vector with the coverage. It is tempting to relate the contact of the Fermi-surface segments of neighboring zones directly with the reconstruction since the two segments are then coupled by $\mathbf{q}=0$. However, the merging is observed to occur at a hydrogen coverage which corresponds to a coverage of only 0.2–0.3 monolayer.²⁴ It is apparent then, because of the low coverage at which segments of the Fermi surface actually merge, that the connection between the reconstruction and the change in Fermi-surface morphology is not singular as one is tempted to assume. Simply on the basis of our data we cannot draw any conclusions regarding this question; ultimately, the answer must await theoretical interpretation.

The data in Figs. 2 and 3 could presumably be coupled to first-principles calculations to provide useful information about the static properties of this surface. For example, it may be possible to deduce information about the hydrogen adsorption site.²⁵ These data also have implications concerning the coupling between low-energy elementary excitations and the electron-hole pair continuum. For instance, one can predict damping of the zone-center hydrogen phonon excitations polarized normal to the surface. This speculation results from an assumed linkage between the hydrogen-layer adsorption distance and the work-function change,^{26,27} coupled with the relationship observed here between the work-function change and the size of the electron pocket. Vibrational motion of the hydrogen layer normal to the surface would then be coupled to, and damped by, intraband excitations in the electron-hole pair continuum. Further computational input will be required to predict the magnitude of this coupling.

Coupling of the type we suggest here is not without precedent. It is consistent with the general concepts put forth by Persson and Ryberg²⁸ and by Langreth²⁹ who have considered how electron-hole pair excitations coupled to surface vibrations will affect the experimentally observed adsorbate vibrational mode line shape and width. A similar idea invoking interband excitations has been proposed to explain the observed damping of the overtone of the hydrogen wag mode on W(001).^{30,31} Our speculation for H/W(110) differs only in detail, and one might expect that a comparable line shape would be apparent in infrared and specular electron-energy-loss studies of hydrogen on W(110).

Finally, there are many finite-wave-vector screening anomalies which can be predicted from the data of Fig. 2. These can occur when segments of the Fermi surface are nearly parallel to one another.³² Both intraband and interband excitations may result in such anomalies. Examples of segments which may produce anomalies occur along $\bar{\Delta}$ and $\bar{\Sigma}$ ($\bar{\Sigma} \equiv \bar{\Gamma}-\bar{H}$, see Fig. 2) in the vicinity of 0.9 and 1.4 \AA^{-1} , respectively. In both of these regions the electron and hole orbits are nearly parallel over a range of k_{\parallel} and are separated by about 0.3 \AA^{-1} . One might, therefore, expect that coupling of a phonon of this wave vector to the electron-hole continuum would cause Kohn anomalies to exist in the dispersion relations of the surface phonon modes. Again, lacking further theoretical treatment, we cannot predict the strength of the coupling between the phonon modes and the electron-hole pair continuum. However, the fact that the chromium-group metals exhibit pronounced Fermi-surface-induced anomalies in their bulk phonon dispersion relations³² suggests that similar anomalies may occur at the surface. However, the coupling of the bulk electron and hole octahedron, which is believed to be responsible for the antiferromagnetic behavior of Cr,³² does not have a direct surface analog. This is due to the size and shape of the hole orbit observed centered at \bar{N} which considerably differs from that of the bulk hole octahedron centered at the H point. It is important to note that a theoretical treatment of such coupling in the vicinity of $\bar{\Sigma}$ must include the spin-orbit interaction since the separation of the bulk electron and hole orbits along $\bar{\Delta}$ results directly from the spin-orbit-induced splitting of the Δ_5 state.³³

We would like to acknowledge the assistance of Sanjay Dhar in the performance of some of the experimental work presented here. This work was carried out in part at the National Synchrotron Light Source at Brookhaven National Laboratory which is supported by the U.S. Department of Energy, Division of Materials Science and the Division of Chemical Sciences. Financial support from the U.S. DOE under Grant No. DE-FG06-86ER45275 and from the American Chemical Society Petroleum Research Fund is gratefully acknowledged. The work of S.D.K. was supported by the National Sci-

ence Foundation and the Alfred P. Sloan Foundation.

^(a)Current address: Brookhaven National Laboratories, National Synchrotron Light Source, Bldg. 725A/U3, Upton, NY 11973.

¹L. R. Testardi and R. R. Soden, *Phys. Rev.* **158**, 581 (1967).

²T. Holstein, R. E. Norton, and P. Pincus, *Phys. Rev. B* **8**, 2649 (1973).

³P. T. Coleridge, in *Electrons at the Fermi Surface*, edited by M. Springford (Cambridge Univ. Press, Cambridge, 1980).

⁴D. Shoenberg and P. J. Stiles, *Proc. Roy. Soc. London A* **281**, 62 (1964).

⁵R. F. Girvan, A. V. Gold, and R. A. Phillips, *J. Phys. Chem. Solids* **29**, 1485 (1968).

⁶J. F. Koch, in *Solid State Physics—Electrons in Metals*, edited by J. F. Cochran and R. R. Haering (Gordon and Breach, New York, 1968), Vol. 1.

⁷A. M. Afanas'ev and Yu. Kagan, *Zh. Eksp. Teor. Fiz.* **43**, 1456 (1962) [*Sov. Phys. JETP* **16**, 1030 (1963)].

⁸M. J. Rice and S. Strässler, *Solid State Commun.* **13**, 125 (1973).

⁹J. C. Campuzano, D. A. King, C. Somerton, and J. E. Inglesfield, *Phys. Rev. Lett.* **45**, 1649 (1980).

¹⁰X. W. Wang, C. T. Chan, K. M. Ho, and W. Weber, *Phys. Rev. Lett.* **60**, 2066 (1988).

¹¹D. King, *J. Phys. C* **14**, 3099 (1981).

¹²W. Kohn, *Phys. Rev. Lett.* **2**, 393 (1959).

¹³G. Benedek, G. Brusdeylins, C. Heimlich, L. Miglio, J. G. Skofronick, J. P. Toennies, and R. Vollmer, *Phys. Rev. Lett.* **60**, 1037 (1988).

¹⁴U. Harten, J. P. Toennies, C. Wöll, and G. Zhang, *Phys. Rev. Lett.* **55**, 2308 (1985).

¹⁵J. W. Chung, S. C. Ying, and P. J. Estrup, *Phys. Rev. Lett.*

56, 749 (1986).

¹⁶M. Altman, J. W. Chung, P. J. Estrup, J. M. Kosterlitz, J. Prybyla, D. Sahu, and S. C. Ying, *J. Vac. Sci. Technol. A* **5**, 1045 (1987).

¹⁷(a) J. A. Becker, E. J. Becker, and P. J. Brandes, *J. Appl. Phys.* **32**, 411 (1961); (b) P. W. Tamm and L. D. Schmidt, *J. Chem. Phys.* **54**, 4775 (1971).

¹⁸S. D. Kevan, *Rev. Sci. Instrum.* **54**, 1441 (1983).

¹⁹P. Thiry, P. A. Bennett, S. D. Kevan, W. A. Royer, E. E. Chaban, J. E. Rowe, and N. V. Smith, *Nucl. Instrum. Methods Phys. Res., Sect. A* **222**, 85 (1984).

²⁰R. H. Gaylord and S. D. Kevan, *Phys. Rev. B* **36**, 9337 (1987).

²¹R. H. Gaylord, K. Jeong, S. D. Kevan, and M. Weinert (to be published).

²²Coverage calibrations were obtained by using the work-function versus coverage data of B. D. Barford and R. R. Rye, *J. Chem. Phys.* **60**, 1046 (1974).

²³R. H. Gaylord and S. D. Kevan, *Phys. Rev. B* **37**, 8491 (1988).

²⁴R. H. Gaylord, K. Jeong, and S. D. Kevan, in *Proceedings of the Thirty Fifth National Symposium of the American Vacuum Society* (to be published).

²⁵K. Jeong, R. H. Gaylord, and S. D. Kevan, *Phys. Rev. B* **39**, 2973 (1989).

²⁶P. J. Feibelman and D. R. Hamann, *Surf. Sci.* **182**, 411 (1987).

²⁷R. Biswas and D. R. Hamann, *Phys. Rev. Lett.* **56**, 2291 (1986).

²⁸B. N. J. Persson and R. Ryberg, *Phys. Rev. Lett.* **48**, 549 (1982).

²⁹D. C. Langreth, *Phys. Rev. Lett.* **54**, 126 (1985).

³⁰Y. J. Chabal, *Phys. Rev. Lett.* **55**, 845 (1985).

³¹J. E. Reutt, Y. J. Chabal, and S. B. Christman, *Phys. Rev. B* **38**, 3112 (1988).

³²T. M. Rice and B. I. Halperin, *Phys. Rev. B* **1**, 509 (1970).

³³L. F. Mattheiss and R. E. Watson, *Phys. Rev. Lett.* **13**, 526 (1964).